Selective ^{1}H-^{1}H Distance Restraints in Fully Protonated Proteins by Very Fast Magic-Angle Spinning Solid-State NMR

*Mukul Jain,[a§] Daniela Lalli,[b§] Jan Stanek,[b] Chandrakala Gowda,[a] Satya Prakash,[a] Tom S. Schwarzer,[c] Tobias Schubeis,[b] Kathrin Castiglione,[c] Loren B. Andreas,[d] P.K. Madhu,[a,e] Guido Pintacuda[b] and Vipin Agarwal[a]**

[a]TIFR Centre for Interdisciplinary Sciences, Tata Institute of Fundamental Research, 21 Brundavan Colony, Narsingi, Hyderabad 500 075, India

[b]Centre de RMN à Tres Hauts Champs, Institut des Sciences Analytiques (UMR 5280 – CNRS, ENS Lyon, UCB Lyon 1), Université de Lyon, 5 rue de la Doua, 69100 Villeurbanne, France

[c]Institute of Biochemical Engineering, Technical University of Munich, Boltzmannstraße 15, D-85748 Garching, Germany

[d]Max Planck Institute for Biophysical Chemistry, Am Fassberg 11, D-37077 Göttingen, Germany

[e]Department of Chemical Sciences, Tata Institute of Fundamental Research, Homi Bhabha Road, Colaba, Mumbai 400 005, India

§ **Both these authors contributed equally**

Corresponding Author

*vipina@tifrh.res.in

Supporting Information

1. Spin Simulations

Spin-System and parameters used in the numerical simulation of the BASS-SD mixing scheme shown in Figure 1 of the main text and Figure S1 of the supporting information.

Eight protons spin simulations:

The eight spin system simulations were carried out using a homonuclear spin system at, 850MHz and 100 kHz MAS frequency. The 8 spins were namely 1) $2H^{N}$, 2) $7H^{N}$, 3) $5H^{N}$, 4) $1H^{N}$, 5) $6H^{\alpha}$, 6) $3H^{\alpha^1}$, 7) $4H^{\alpha^2}$ and 8) $8H^{ali}$. The value of isotropic chemical shifts, CSA tensors and the homonuclear dipolar couplings are summarized in the table below. All plots were simulated with 300-crystal orientations. Simulations do not include any RF field inhomogeneity and the RF-field amplitudes were varied in a range from 3 to 25 kHz.

Table S1. Description of the 8-spin system used to follow polarization transfer in case of BASS-SD simulations.

Dipolar coupling spin pair (H_i,H_j)	$\delta^{D}{}_{H}{}^{i}{}_{H}{}^{j}$	$\alpha_{H}{}^{i}{}_{H}{}^{j}$	$\beta_{H}{}^{i}{}_{H}{}^{j}$	$\gamma_{H}{}^{i}{}_{H}{}^{j}$
1-2	-3959.4	0	0.0	0.0
1-3	-12184	0	-127.67	-85.043
1-4	-11303	0	-21.491	-218.630
1-5	-10687	0	-81.025	-165.140
1-6	-10114	0	-119.15	-277.300
1-7	-21054	0	-63.039	-238.320
1-8	-6757.4	0	-74.909	-303.090
2-3	-3254.4	0	104.800	194.670
2-4	-11347	0	156.590	95.320
2-5	-1345.6	0	57.253	42.917
2-6	-1237.2	0	169.170	232.400
2-7	-2082.5	0	86.303	230.150
2-8	-7175.4	0	98.049	233.030
3-4	-3146	0	-178.870	-78.724
3-5	-20032	0	-19.044	-39.491
3-6	-1594.4	0	-11.446	-145.650
3-7	-1982.9	0	-80.707	-131.690
3-8	-2563.3	0	-137.430	-226.040
4-5	-2747.6	0	34.565	49.995
4-6	-6173.5	0	125.330	33.775
4-7	-7538.2	0	94.573	190.000
4-8	-3660.6	0	155.010	174.550
5-6	-3019.2	0	-93.609	-125.180
5-7	-2298.8	0	-27.000	-210.990
5-8	-1195.2	0	-47.186	-16.003
6-7	-39337	0	123.8	129.320
6-8	-1705.5	0	132.54	142.090
7-8	-5425.2	0	-3.524	-119.110

Atom (H_i)	$\delta^{CS(i)}{}_{Iso}$	$\delta^{CS(i)}{}_{Aniso}$(Hz)	η	$\alpha_{H}{}^{i}$	$\beta_{H}{}^{i}$	$\gamma_{H}{}^{i}$
1	8.97	11985	0.95	116.6	122.2	228.9
2	8.67	9350	0.85	-149.9	46.2	-220.8
3	9.21	12835	0.90	97.9	129.8	188.1
4	7.71	12155	1.00	-139.0	167.9	-350.2
5	3.72	8000	0.83	70.8	120.9	266.9
6	4.12	7000	0.99	-135.9	43.7	-159.3
7	3.47	8400	0.87	123.0	126.7	159.2
8	0.73	3000	0.90	-76.4	48.6	-70.9

Here the distance between the amide protons were artificially doubled while the distance between the source amide protons and aliphatic protons was kept constant. Even under such condition the polarization exchange takes places only within amide protons.

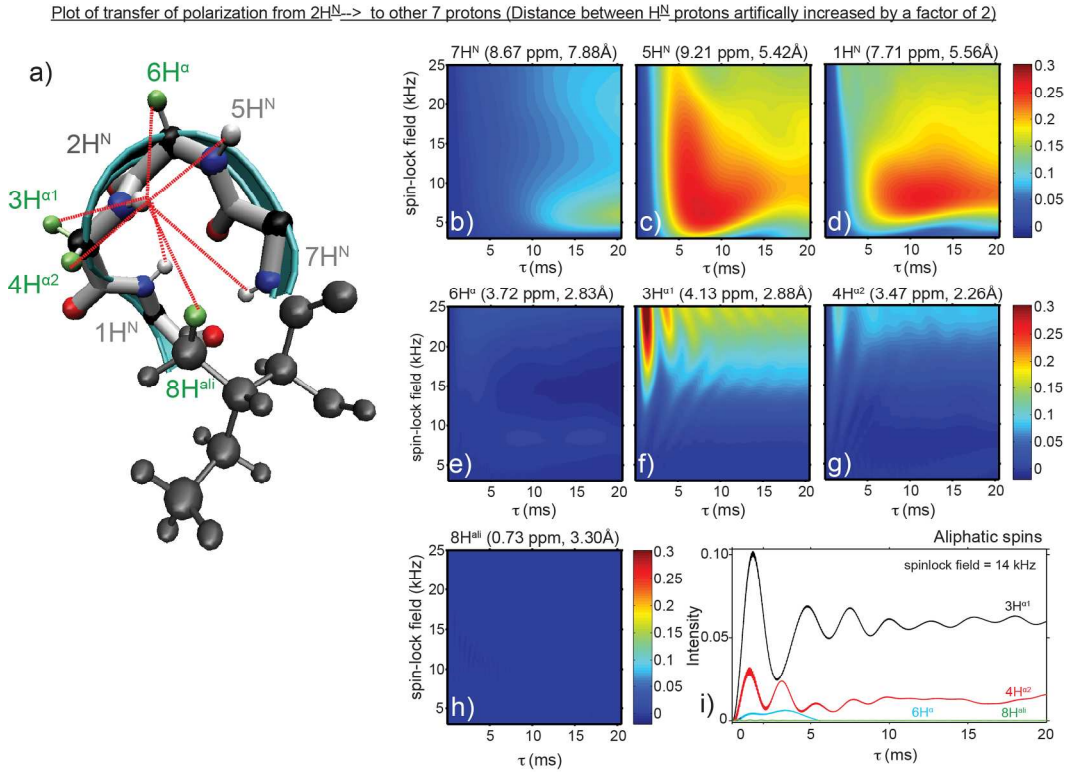

Figure S1. Plot shows the simulated build up polarization for a system of eight proton spins selected from the crystal-structure of Ubiquitin in presence of BASS-SD mixing. In addition to $2H^N$ (source spin) the spin system comprises three closest HN protons to $2H^N$ and four closest aliphatic protons. In comparison to the Figure 1 (in the main text), the distance between the amide protons was doubled while keeping the distance between the aliphatic and the source spin constant $2H^N$ a) Simulated spin system extracted from the crystal structure. The green and white spheres represent aliphatic and amide protons used for simulation. b-h) The build-up of polarization as a function of mixing time and spin-lock field strength for different spins. The numbers in the brackets indicate isotropic chemical shifts and distance from $2H^N$ b) $7H^N$ c) $5H^N$ d) $1H^N$ e) $6H^{\alpha}$ f) $3H^{\alpha 1}$ g) $4H^{\alpha 2}$ h) $8H^{ali}$. i) Overlay of build-up profile for the four aliphatic protons at spin-lock field of 14 kHz.

2. Sample Preparation

Uniformly ^{13}C,^{15}N-labeled GB1 was expressed in *Escherichia coli*, purified, and precipitated as described previously.[1] This is briefly recapitulated here.

AlkL from *Pseudomonas putida* was expressed, purified and refolded as described elsewhere.[2]

AlkL from *Pseudomonas putida* F1 was expressed in *Escherichia coli* C43 grown in M9 minimal medium (4.8 g L^{-1} Na_2HPO_4, 3 g L^{-1} KH_2HPO_4, 0.5 g L^{-1} NaCl, 0.12 g L^{-1} $MgSO_4$, 1 g L^{-1} $^{15}NH_4Cl$, 0.03 g L^{-1} $CaCl_2$, 10 mg L^{-1} EDTA, 1.5 mg L^{-1} $FeCl_3 \cdot 6H_2O$, 1 µg L^{-1} thiamine, 1 µg L^{-1} biotin,150 µg L^{-1} $CoCl_2 \cdot 6H_2O$, 30 µg L^{-1} $CuSO_4 \cdot 5H_2O$, 30 µg L^{-1} $CuSO_4 \cdot 5H_2O$, 150 µg L^{-1} H_3BO_4, 180 µg L^{-1} KI, 120 µg L^{-1} $MnCl_2 \cdot 4H_2O$, 60 µg L^{-1} $NaMoO_4 \cdot 6H_2O$, 23 µg L^{-1} $NiCl_2 \cdot 6H_2O$, 120 µg L^{-1} $ZnSO_4 \cdot 7H_2O$; pH 7.2) supplemented with 50 mg L^{-1} ampicillin and 3 g L^{-1} ^{13}C-glucose at 37 °C and 250 rpm until a cell density (OD_{600}) of 0.6-0.8 was reached. Protein expression was induced by the addition of 1 mM IPTG and cells were harvested by centrifugation after another 4 h of expression. Purification and refolding was performed as described elsewhere[2]. Using a reduced feed rate of 1 µL min^{-1} and a final protein concentration of 3 g L^{-1}, >90 % of the protein could be refolded in the first step. Residual misfolded protein was removed by a subsequent ion exchange step. To this end, the refolded protein was excessively dialyzed against 10 mM Tris-HCL pH 8 supplemented with 0.05 % w/v *N,N*-dimethyldodecylamine *N*-oxide (LDAO), applied to a 1 mL capto Q AEX column (GE Healthcare) and eluted into the same buffer at a NaCl concentration of 300 mM. For reconstitution into lipids, the buffer was then exchanged to 20 mM sodium phosphate pH 7, supplemented with 10 mM aspartic acid, 10 mM glutamic acid and 2 % w/v octyl glucoside (OG) using a desalting column (GE Healthcare). Deuterated (d54) DMPC (Avanti) was added in a protein - lipid ratio of 2:1 (w/w) and the detergent was removed by dialysis. AlkL in lipid bilayers was directly centrifuged into a 0.7 mm MAS rotor.

3. NMR Spectroscopy

All experiments were carried out on a Bruker Avance III 800 MHz standard bore spectrometer operating at a static field of 18.8 T, equipped with a triple channel H, C, N, 0.7 mm probe, at a MAS frequency $\omega_r/2\pi$ of 111.111 kHz. Sample temperature was maintained at about 295K using a Bruker cooling unit with regulated N_2 gas directed at the rotor. The temperature of this gas measured just before reaching the sample was 270K.

The non-selective pulses were set to 2.5 µs at 100 kHz RF-field amplitude (^{1}H), 4.5 µs at 55.5 kHz RF-field amplitude (^{15}N) and 3.5 µs at 71.4 kHz RF-field amplitude (^{13}C).

The ^{1}H-^{15}N and ^{1}H-^{13}C cross-polarization (CP) were performed using a constant RF frequency applied to ^{15}N and ^{13}C and a pulse linearly ramped from 90% to 100%; they were optimized around nutation frequencies of 4/3 ω_r for proton, and 1/3 ω_r for carbon and nitrogen. CP contact times of 1 ms and 400 µs were used for the ^{1}H-^{15}N and ^{15}N-^{1}H CP, respectively. Different CP contact times were used to select the H^α and the methyl resonances: 500 µs and 100 µs for the ^{1}H-^{13}C and ^{13}C-^{1}H CP, respectively ((H)C$H^\alpha H^\alpha$); 950 µs and 600 µs for the ^{1}H-^{13}C and ^{13}C-^{1}H CP, respectively ((H)C(H)(H)CH^{meth} with BASS-SD and RFDR mixing schemes). To uniformly transfer magnetization within the proton nuclei located in the bandwidth of interest, an adiabatic amplitude-modulated tangential shape was applied (having a better performance than a rectangular pulse), as listed in table S2. The tangent amplitude modulation was $A(x)=1 + 0.2 \tan[2\alpha(x-0.5)]/\tan(\alpha)$, where a=1.4 and x varies from 0 to 1.

Low power WALTZ-16 decoupling[3] of 10 kHz was applied for heteronuclear decoupling. swept low-power TPPM (SW_f-TPPM) decoupling[4] was used during ^{13}C, ^{15}N chemical shift evolution with a ^{1}H RF frequency of 27.7 kHz and a pulse-length duration of 9 μs. DIPSI-2[5] with RF of $\gamma B_1/2\pi$=20 kHz was used for ^{13}C decoupling during proton acquisition due to the presence of homonuclear ^{13}C-^{13}C J-couplings. Suppression of solvent signals[6] was applied using the MISSISSIPPI scheme[7] without the homospoil gradient for 200 ms. The inter-scan recycle delay was 0.8-1 s.

Spectra were apodized in each dimension with 90-degree shifted squared sine-bells ('Qsine 2' in Bruker Topspin), and zero-filled to at least twice the number of points in the indirect dimensions. Experimental parameters for the NMR spectra acquired on GB1 and AlkL are summarized in Tables S2 and S4. Acquisition and processing parameters specific for each dataset are listed in Tables S3 and S5. Spectra were processed with Topspin3.5, and their analysis was performed CcpNmr Analysis.[8]

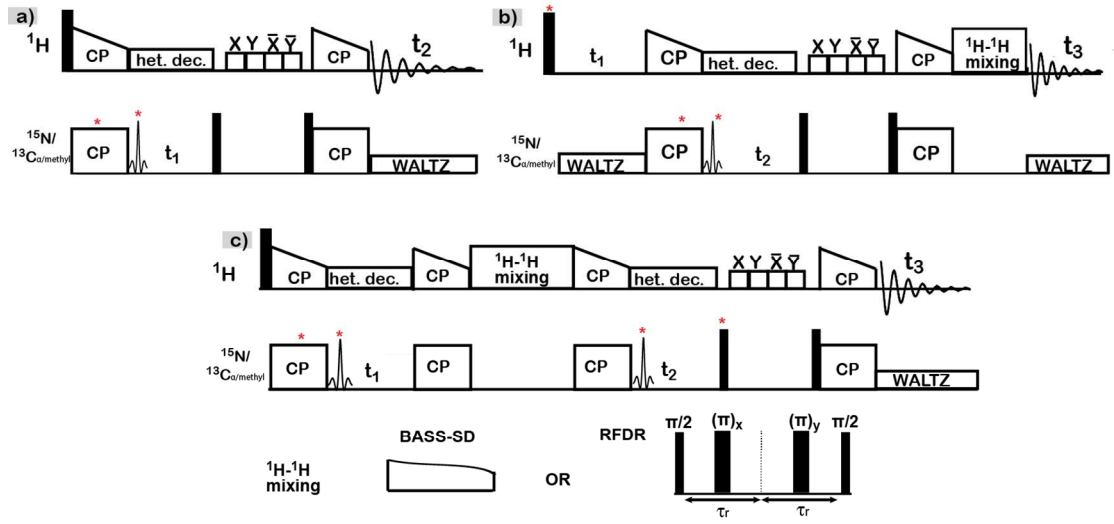

Figure S2. Pulse sequence for ^{1}H detected a) 2D (H)NH b) 3D (H)NHH experiment, c) 3D (H)N(H)(H)NH sequence. The proton mixing was achieved through BASS-SD or RFDR. The shaped pulses are the ReBURP[9] pulses and were used to select out a particular methyl or alpha carbons. In case of ^{15}N experiment the shaped pulses were not applied. The red stars (*) indicate the pulses which were phase cycled. The MISSISSIPPI sequence was used for water suppression while low-power SW_f-TPPM and WALTZ were used to decouple ^{1}H and ^{15}N nuclei during evolution periods.

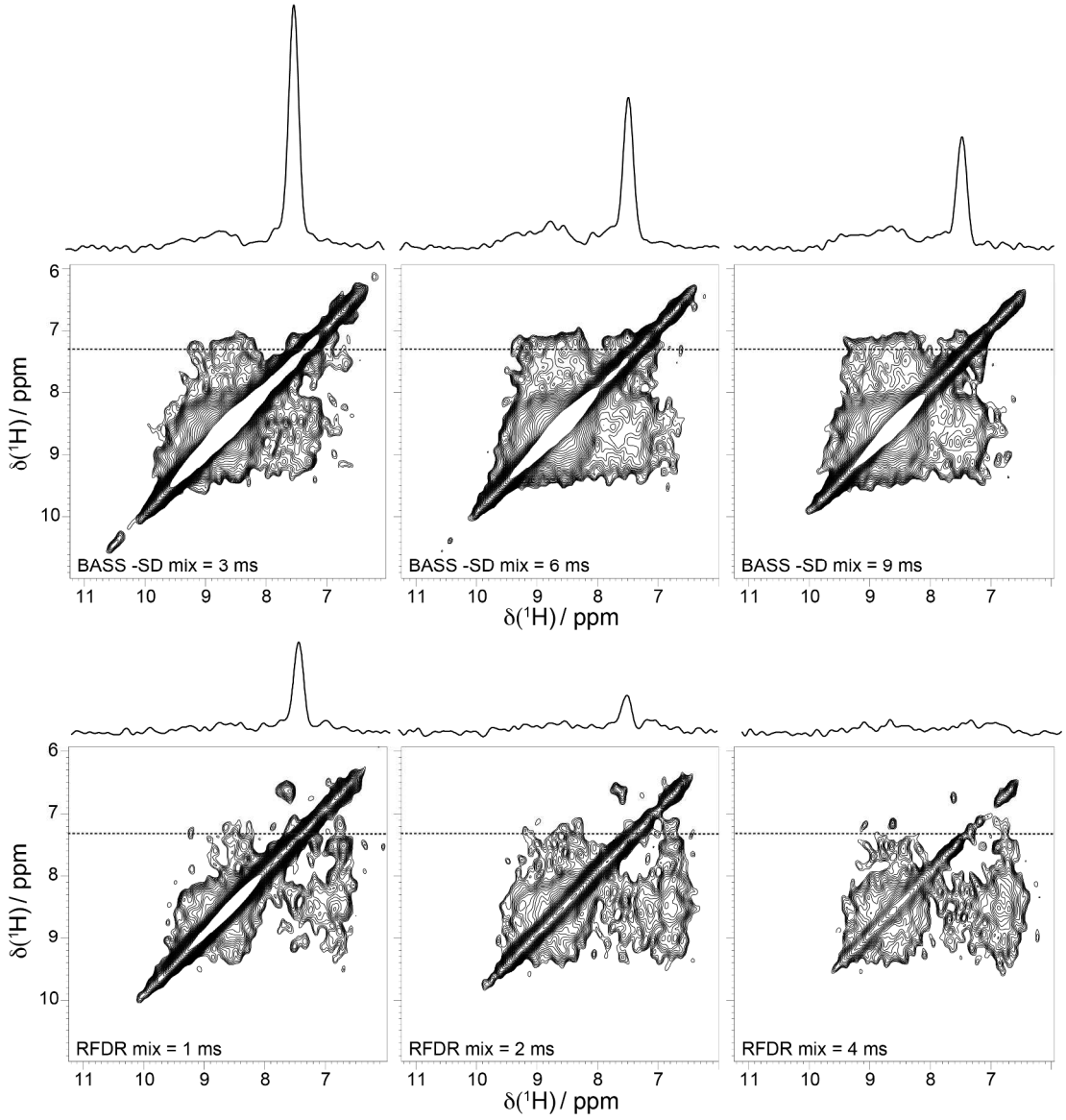

Figure S3. Comparison of the ^{1}H-^{1}H 2D planes of the 3D (H)NHH-BASS-SD (top panels) and RFDR (bottom panels) spectra acquired on the fully protonated U-[^{13}C,^{15}N]-AlkL protein from

Pseudomonas putida, recorded at MAS frequency of 111.11 kHz and 1000 MHz spectrometer. The mixing time was varied to establish the optimal transfer efficiency for the two mixing schemes (3-9 ms for the BASS-SD and 1-4 ms for the RFDR).

Table S2. Experimental parameters for NMR spectra acquired on GB1. The MAS frequency was 111 kHz, the sample temperature was 295K, the magnetic field 800 MHz.

Experiments	H(H)NH BASS-SD	(H)NHH RFDR	(H)CH$^{\alpha}$H$^{\alpha}$ BASS-SD	(H)N(H)(H)NH BASS-SD	(H)N(H)(H)NH RFDR	(H)C(H)(H)CH^{meth} BASS-SD	(H)C(H)(H)CH^{meth} RFDR
^{1}H Offset	9.2 ppm	9.2 ppm	4.6 ppm	9.2 ppm	9.2 ppm	0.8 ppm	0.8 ppm
X Offset	119 ppm	119 ppm	57.6 ppm	117.7 ppm	117.7 ppm	20.6 ppm	20.6 ppm
1st CP							
^{1}H field	152 kHz	152 kHz	148 kHz	147kHz	147kHz	145 kHz	145 kHz
^{1}H shape	Ramp 90-100	Ramp 90-100	Ramp 90-100	Ramp 90-100	Ramp 90-100	Ramp 90-100	Ramp 90-100
X field	37 kHz	37 kHz	36 kHz	39 kHz	39 kHz	41 kHz	41 kHz
X shape	Rectangle	Rectangle	Rectangle	Rectangle	Rectangle	Rectangle	Rectangle
Contact time	1 ms	1 ms	500 µs	1.5 ms	1.5 ms	950 µs	950 µs
2nd CP							
^{1}H field	148 kHz	148 kHz	144 kHz	141 kHz	141 kHz	141 kHz	141 kHz
^{1}H Shape	Ramp 90-100	Ramp 90-100	Ramp 90-100	Ramp 90-100	Ramp 90-100	Ramp 90-100	Ramp 90-100
X field	37 kHz	37 kHz	36 kHz	39 kHz	39 kHz	41 kHz	41 kHz
X shape	Rectangle	Rectangle	Rectangle	Rectangle	Rectangle	Rectangle	Rectangle
Contact time	400 µs	400 µs	100 µs	600 µs	600 µs	600 µs	600 µs
^{1}H-^{1}H mixing							
^{1}H field	4.4 kHz	100 kHz	3.5 kHz	5.5 kHz	200 kHz	2.9 kHz	200 kHz
Mixing Time	5.0 ms	1.15 ms	5.0 ms	5.0 ms	1.0 ms	5.0 ms	1.0 ms
Shape	Rectangle		Rectangle	Tangent up ±20%		Tangent down ±20%	
Decoupling							
WALTZ-16 (^{15}N field)	10 kHz	10 kHz	10 kHz	10 kHz	10 kHz	10 kHz	10 kHz
DIPSI-2 (^{13}C field)	20 kHz	20 kHz	20 kHz	20 kHz	20 kHz	20 kHz	20 kHz
SW-TPPM (^{1}H field)	27.7 kHz	27.7 kHz	27.7 kHz	27.7 kHz	27.7 kHz	27.7 kHz	27.7 kHz

Table S3. Acquisition and processing parameters for the NMR experiments acquired on GB1. The direct proton dimension was sampled to 23 ms but only 15 ms was used for processing. The MAS frequency was 111 kHz.

Spectrum	Max indirect evolution	Sweep width	Scans per point	Experimental time	Interscan delay	Signal/Noise (First FID)	Processing
H(H)NH BASS-SD	3.3 ms (H) 20 ms (N)	6 ppm (H) 40 ppm (N)	12	14 h	1 s	142	90-deg shifted sine-bell squared
(H)NHH RFDR	3.3 ms (H) 20.0 ms (N)	6 ppm (H) 40 ppm (N)	12	14 h	1 s	31	90-deg shifted sine-bell squared
(H)CH$^{\alpha}$H$^{\alpha}$ BASS-SD	4.0 ms (H) 7.5 ms (C)	5.0 ppm (H) 33 ppm (C)	16	14 h	1 s	88	90-deg shifted sine-bell squared
(H)CH$^{\alpha}$H$^{\alpha}$ BASS-SD	5.0 ms (H) 7.5 ms (C)	5.0 ppm (H) 33 ppm (C)	16	18 h	1 s	64	90-deg shifted sine-bell squared
(H)N(H)(H)NH BASS-SD	12.7 ms (N) 20.5 ms (N)	33 ppm (N) 33 ppm (N)	16	27 h	0.8 s	53	90-deg shifted sine-bell squared
(H)N(H)(H)NH RFDR	12.7 ms (N) 20.5 ms (N)	33 ppm (N) 33 ppm (N)	16	27 h	0.8 s	23	90-deg shifted sine-bell squared
(H)C(H)(H)CH^{meth} BASS-SD	10.4 ms (C) 10.4 ms (C)	20 ppm (C) 20 ppm (C)	16	25 h	0.8 s	15	90-deg shifted sine-bell squared
(H)C(H)(H)CH^{meth} RFDR	10.4 ms (C) 10.4 ms (C)	20 ppm (C) 20 ppm (C)	16	25 h	0.8 s	19	90-deg shifted sine-bell squared

Table S4. Experimental parameters for NMR spectra acquired on AlkL. The MAS frequency was 111 kHz, the sample temperature was 305K, the magnetic field 1000 MHz.

Experiments	(H)NHH RFDR	(H)NHH BASS-SD	(H)N(H)(H)NH BASS-SD
^{1}H Offset	8.2 ppm	8.2 ppm	8.2 ppm
X Offset	119.5 ppm	119.5 ppm	119.5 ppm
1st CP			
^{1}H field	149 kHz	149 kHz	149kHz
^{1}H shape	Ramp 90-100	Ramp 90-100	Ramp 90-100
N field	31 kHz	31 kHz	31 kHz
N shape	Rectangle	Rectangle	Rectangle
Contact time	600 µs	600 µs	600 µs
2nd CP			
^{1}H field	146 kHz	146 kHz	146 kHz
^{1}H Shape	Ramp 90-100	Ramp 90-100	Ramp 90-100
N field	31 kHz	31 kHz	31 kHz
N shape	Rectangle	Rectangle	Rectangle
Contact time	300 µs	300 µs	300 µs
^{1}H-^{1}H mixing			

^{1}H field	192 kHz	6.25 kHz	6.25 kHz
Mixing Time	1, 2, 4 ms	3, 6, 9 ms	6.0 ms
Shape		Tangent down ±20%	Tangent down ±20%
Decoupling			
WALTZ-16 (^{15}N field)	10 kHz	10 kHz	10 kHz
SW-TPPM (^{1}H field)	27.7 kHz	27.7 kHz	27.7 kHz

Table S5. Acquisition and processing parameters for the NMR experiments acquired on AlkL. The direct proton dimension truncated at 10 ms was used for processing. The MAS frequency was 111 kHz.

Spectrum	Max indirect evolution	Sweep width	Scans per point	Experimental time	Interscan delay	Processing
(H)(N)HH RFDR	6.0 ms (H)	13.5 ppm (H)	40	1.5 h	0.8 s	60-deg shifted sine-bell squared
(H)(N)HH BASS-SD	6.0 ms (H)	13.5 ppm (H)	40	1.5 h	0.8 s	60-deg shifted sine-bell squared
(H)N(H)(H)NH BASS-SD	9.0 ms (N) 9.0 ms (N)	35 ppm (N) 35 ppm (N)	192	7 days 7 h	0.8 s	60-deg shifted sine-bell squared

4. References

(1) Franks, W. T.; Zhou, D. H.; Wylie, B. J.; Money, B. G.; Graesser, D. T.; Frericks, H. L.; Sahota, G.; Rienstra, C. M. Magic-angle spinning solid-state NMR spectroscopy of the β 1 immunoglobulin binding domain of protein G (GB1): N-15 and C-13 chemical shift assignments and conformational analysis. *J. Am. Chem. Soc.* **2005,** *127*, 12291-12305.
(2) Schwarzer, T. S.; Hermann, M.; Krishnan, S.; Simmel, F. C.; Castiglione, K. Preparative refolding of small monomeric outer membrane proteins. *Protein Expression Purif.* **2017**, 10.1016/j.pep.2017.01.012.
(3) Shaka, A. J.; Keeler, J.; Frenkiel, T.; Freeman, R. An Improved Sequence for Broad-Band Decoupling: WALTZ-16. *J. Magn. Reson.* **1983,** *52*, 335-338.
(4) Mithu, V. S.; Paul, S.; Kurur, N. D.; Madhu, P. K. Heteronuclear Dipolar Decoupling in Solid-State Nuclear Magnetic Resonance Under Ultra-High Magic-Angle Spinning. *J. Magn. Reson.* **2011**, *209* (2), 359–363.
(5) Shaka, A. J.; Lee, C. J.; Pines, A. Iterative Schemes for Bilinear Operators - Application to Spin Decoupling. *J. Magn. Reson.* **1988,** *77*, 274-293.
(6) Paulson, E. K.; Morcombe, C. R.; Gaponenko, V.; Dancheck, B.; Byrd, R. A.; Zilm, K. W. Sensitive high resolution inverse detection NMR spectroscopy of proteins in the solid state. *J. Am. Chem. Soc.* **2003,** *125*, 15831-15836.
(7) Zhou, D. H.; Rienstra, C. M. High-performance solvent suppression for proton detected solid-state NMR. *J. Magn. Reson.* **2008,** *192*, 167-72.

(8) Vranken, W. F.; Boucher, W.; Stevens, T. J.; Fogh, R. H.; Pajon, A.; Llinas, M.; Ulrich, E. L.; Markley, J. L.; Ionides, J.; Laue, E. D. The CCPN data model for NMR spectroscopy: development of a software pipeline. *Proteins* **2005,** *59*, 687-96.
(9) Geen, H.; Freeman, R. Band-Selective Radiofrequency Pulses. *J. Magn. Reson.* **1991,** *93*, 93-141.